A Linear Programming-Driven MCDM Approach for Multi-Objective Economic Dispatch in Smart Grids

Beatrice Lazzerini and Francesco Pistolesi
Department of Information Engineering, University of Pisa
Largo Lucio Lazzarino, 1 - 56122, Pisa, Italy
Email: {b.lazzerini, f.pistolesi}@iet.unipi.it

***Abstract*—This paper presents a novel approach to deal with the multi-objective economic dispatch problem in smart grids as a multi-criteria decision making (MCDM) problem, whose decision alternatives are dynamically generated. Four objectives are considered: emissions, energy cost, distance of supply, and load balancing. Objectives are preliminarily preference-ranked through a fuzzy version of the analytic hierarchy process (AHP), and then classified into two categories of importance. The more important objectives form the objective function of a linear programming (LP) problem, whose solution (driving solution) drives the generation of Pareto-optimal alternative configurations of power output of the generators. The technique for order of preference by similarity to ideal solution (TOPSIS) is used to automatically select the most suitable power output configuration, according to initial preferences, derived with fuzzy AHP. The effectiveness of our approach is validated by comparing it to the weighted sum (WS) method, by simulating 40 different operating scenarios on a prototype smart microgrid.**

***Index Terms*—Decision making; Economic dispatch; Fuzzy sets; Linear programming; Microgrids; Multi-objective optimization; Smart grids.**

NOMENCLATURE

$\mathcal{B}$, $\mathcal{L}$	Set of buses/lines
$\mathcal{G}$, $\mathcal{A}$	Set of generators/active prosumers
$\mathcal{C}$	Set of central controllers
$\mathcal{I}$	Set of central controllers of islanded microgrids
$\mathcal{B}_i^{\rightarrow}$	Set of buses absorbing power directly from bus i
$\mathcal{B}_i^{\leftarrow}$	Set of buses injecting power directly into bus i
(i,j)	Line connecting bus i to bus j
g_{ij}	Conductance of line (i,j)
x_{ij}, b_{ij}	Reactance/susceptance of line (i,j)
V_i	Voltage magnitude at bus i
θ_{ij}	Phase angle difference between bus i and bus j
p_{ij}, q_{ij}	Active/reactive power flow on line (i,j)
ℓ_{ij}	Power losses of line (i,j)
$\underline{P}_i, \overline{P}_i$	Lower/upper active power limit of generator i
d_{ij}	Distance of bus i from bus j
$\overline{\varphi}_{ij}$	Upper power flow limit of line (i,j)

I. INTRODUCTION

The ever-increasing demand for energy, coupled with the reduction of the traditional energy sources, has caused the change of the energy distribution grid from the traditional electricity network, which passively carries energy from few large power generators to a large number of small and medium consumers, to the so-called *smart grid*, which allows two-way flows of electricity and information. A smart grid is based on distributed generation, and communication technologies and standards [1] for intelligent integration of all connected users, in order to distribute energy in an efficient [2] and secure way [3], [4]. Smart grid customers may both consume and produce energy (so-called *prosumers*), and may directly contribute to control and optimize the global system [5]. Environmental impact of the electric system is also reduced thanks to the increased use of renewable energy (mainly wind and solar).

For improved efficiency and management, the energy system is expected to become a set of almost independent smart subsystems or microgrids. A *smart microgrid* is a self-managed localized grouping of energy consumers, producers and prosumers. Typical energy sources are solar panels on the roofs of buildings and small wind turbines. A microgrid is characterized by medium or low voltage level for energy distribution. Examples of microgrid are a village, a part of a town, or an industry site. A microgrid may be connected to the traditional, wide-area power grid, or to other microgrids, or may even function autonomously. In the last case, the microgrid is said to be *islanded*. An islanded microgrid is (intentionally) disconnected from the main grid, hence voltage and frequency are no longer controlled by the utility grid.

Consequently, within the islanded microgrid, a voltage and frequency control strategy has to be guaranteed [6], and the distributed generation has to be managed to meet the needs of the consumers, by possibly performing intelligent load shedding policies [7].

The ability to isolate microgrids lets a microgrid be seen as a single entity connected to the main grid through the transmission and distribution system: at any instant, from the main grid perspective, the microgrid will be regarded as either a consumer or a producer. This means that microgrids can be seen as building blocks of a wider power grid. In other words, the smart grid, which is regarded as the next generation power grid, can be modeled as a hierarchical structure in which two-way flows of electricity and information travel between the high-voltage network and smart microgrids at different hierarchical levels. From a technical point of view, three main

systems can be singled out in a smart (micro)grid, namely, the smart infrastructure system (concerned with both energy generation, transmission and distribution, and information metering, management and transmission), the smart management system (concerned with control tasks, e.g., emission control, cost reduction, or supply and demand balance) and the smart protection system (concerned with reliability, security and privacy issues).

As far as the smart management system is concerned, simultaneous optimization of more than one objective is implied, in particular, reduction of the environmental impact (also referred to as the pollution level), cost minimization, demand and supply balancing, and reduction of the amount of energy lost in transmitting electricity. Each of these objectives can be singularly achieved, e.g., respectively, by an extensive use of renewable sources, by varying the energy price over time, by reducing the peaks of energy consumption (e.g., by performing task scheduling and temporarily turning off non-essential devices [8]) so as to achieve a load profile over time as constant as possible, and by increasing the closeness between energy production and consumption [9]. In general, however, the problem can be regarded as a multi-criteria decision making problem. It is well-known that usually there does not exist a single solution to such a problem that simultaneously optimizes all the objectives.

Actually, most of the papers found in the literature deal separately with either energy efficiency improvement [10], [11], demand profile shaping [12]–[15], utility and cost optimization [16]–[20], or emission control [21]. Some works try to achieve the best trade-off between two objectives, e.g., in [22] the authors try to minimize both cost and emission simultaneously; while in [23] and [24], the demand and supply balance is improved while minimizing the energy costs.

In this paper we propose an approach to multi-objective economic dispatch in the smart grid taking the following four criteria into account: environmental impact, cost of the energy, distance of supply, and load balancing.

To solve this problem we perform the following two steps:

1) *generation of alternative solutions*: in this step, as there are more conflicting objectives to be optimized simultaneously, a finite set of possible solutions (or alternatives) will be generated;
2) *solution selection*: in this step, the possible solutions are compared with respect to different, typically conflicting, objectives (or criteria) in order to select the preferred solution.

We adopt linear programming (LP) to control the generation of alternative solutions, and an integration of a fuzzy version of the analytic hierarchy process (AHP) and the technique for order of preference by similarity to ideal solution (TOPSIS) for the solution selection. In particular, fuzzy AHP and TOPSIS are used, respectively, to prioritize the criteria and to evaluate the alternatives. As a preliminary step, we model a smart grid as a radial directed graph [25].

The rest of this paper is organized as follows. Section II introduces multi-criteria decision making; in Section III we describe the multi-criteria decision making techniques we use in the paper; Section IV contains an overview of the DC power flow model with energy losses; in Section V our model of the smart grid is described; in Section VI we formalize multi-objective economic dispatch as a linear programming-driven multi-criteria decision making problem, then we introduce the technique for alternative generation, and the resolution strategy; Section VII contains the results of the experiments we made on a prototype smart grid. Finally, in Section VIII, we draw the conclusions of our work.

II. Multi-criteria decision making

A. Overview

Multi-criteria decision making (MCDM) is a branch of operations research. MCDM refers to making decisions considering multiple and potentially conflicting criteria. MCDM problems can be classified into two classes: multi-objective decision making (MODM) and multi-attribute decision making (MADM) problems. MODM is also known as multi objective optimization (MOO).

B. Multi-objective optimization

MOO problems are optimization problems wherein multiple objective functions are simultaneously intended to be optimized. In mathematical terms, a multi-objective optimization problem can be written as

$$\text{Minimize } f = [f_1(x), f_2(x), \ldots, f_t(x)] \tag{1}$$

subject to:

$$g_i(x) \leq 0, \quad i = 1, \ldots, m \tag{2}$$

$$h_j(x) = 0, \quad j = 1, \ldots, n \tag{3}$$

where $t \geq 2$ is the number of objectives, m and n are, respectively, the number of inequality and equality constraints, that define the feasible region X. The global objective function $f : X \rightarrow \mathbb{R}^t$ is a vector-valued function defined as $f(x) = [f_1(x), \ldots, f_t(x)]^T$, containing all the objective functions to be optimized. Each element $x \in X$ is a feasible solution. In general, in an MOO problem there does not exist a feasible solution minimizing all the objective functions simultaneously. Therefore, the concept of *Pareto-optimal solution* is introduced. A Pareto-optimal solution is a particular feasible solution that cannot be improved with respect to any objective without degrading at least one of the other objectives. More rigorously, a feasible solution $x_1 \in X$ is said to (Pareto-)dominate another solution $x_2 \in X$, if $f_i(x_1) \leq f_i(x_2) \, \forall i \in \{1, \ldots, t\}$, and $f_j(x_1) < f_j(x_2)$ for at least an index $j \in \{1, \ldots, t\}$. A solution $x_1 \in X$ is Pareto-optimal if there does not exist another solution that dominates it. The set of Pareto-optimal solutions in the objective space is called *Pareto front*.

The WS method requires the expert to express a set of weights $W = (w_1, \ldots, w_t)$, one for each objective function,

in order to derive the following aggregate objective function to be optimized:

$$F = \sum_{i=1}^{t} w_i f_i(x). \quad (4)$$

If all the weights are positive, then minimizing (4) provides a sufficient condition for Pareto optimality of the solution [26].

C. Multi-attribute decision making

An MADM problem is characterized by a goal, a set of attributes (or criteria) and a set of alternatives. In the following, as is typical in the literature, we will refer to MADM just as MCDM. Criteria and alternatives are called *elements*. Alternatives represent different choices available to the decision maker. Criteria are like different perspectives from which the alternatives can be viewed. The goal consists in finding the best alternative with respect to all the criteria. Most MCDM methods associate a weight with each criterion to express the decision maker's relative preference of the criteria themselves. Weights can be directly chosen by the decision maker, or they can be the result of a ranking technique [27].

III. Multi-criteria decision making techniques

A. Analytic Hierarchy Process (AHP)

AHP is a technique which organizes an MCDM problem as a hierarchy whose uppermost level contains the goal, intermediate levels contain criteria, sub-criteria, etc., and the lowest level contains the alternatives [28]. Since criteria might be divided into sub-criteria, and sub-criteria into sub-subcriteria and so on, we will refer to a lowest-level sub-criterion as a *lowest sub-criterion*. AHP ranks criteria with respect to each other, with reference to their parent in the hierarchy. Alternatives are ranked according to each lowest sub-criterion. AHP requires to build a pairwise comparison matrix for each level of the hierarchy, by comparing elements sharing the same parent. Given two elements i and j, the result of a pairwise comparison is a coefficient m_{ij} estimating the preference of i over j. The coefficients, called *preference weights*, are expressed by the Saaty's scale of preference, shown in Table I.

An $n \times n$ pairwise comparison matrix M is said to be *consistent* if $m_{ij} = m_{ik}m_{kj}, \forall i, j, k \in \{1, \ldots, n\}$. It has been proved [29] that the principal eigenvector is a representation of the element priorities derived from a consistent pairwise comparison matrix. A preference expresses the importance of an element with respect to the ones sharing the same parent in the hierarchy. In order to obtain global weights, i.e., the weight of each element with respect to the root element of the hierarchy, the preference of each element is multiplied by the ones related to its ancestors in the hierarchy, until the uppermost level is reached. The decisional problem is solved by choosing the alternative having the greatest global weight. Whenever an $n \times n$ pairwise comparison matrix is consistent, its principal eigenvalue λ_{max} is equal to n. In order to check if each comparison matrix M is consistent, AHP computes the *consistency index* $CI \triangleq \frac{\lambda_{max}-n}{n-1}$, and compares it with a *random index* (RI) obtained by the mean of the consistency indexes of many reciprocal pairwise comparison matrices of the same order of M, whose elements are randomly generated according to a uniform probability distribution. This comparison is performed by computing the *consistency ratio* $CR = \frac{CI}{RI}$. If $CR \leq 0.1$, the coherence requirement is met, otherwise AHP requires the expert to increase the coherence of his/her judgements.

TABLE I
Saaty's scale of preference

Preference weight m_{ij}	Explanation
1	Equally preferred
3	Moderately preferred
5	Strongly preferred
7	Very Strongly preferred
9	Extremely preferred
2, 4, 6, 8	Intermediate values (compromises)

B. Fuzzy AHP

Human judgements are usually affected by imprecision and vagueness. Fuzzy set theory [30] can effectively deal with this problem. A fuzzy set is defined as $F = \{(x, \mu_F(x)), x \in \mathbb{U}\}$, where $\mathbb{U}$ is the universe of discourse and μ_F is the *membership function* such that $x \mapsto \mu_F(x)$, where $\mu_F(x) \in [0, 1]$. The set $\{x : \mu_F(x) > 0\}$ is the *support* of the fuzzy set F.

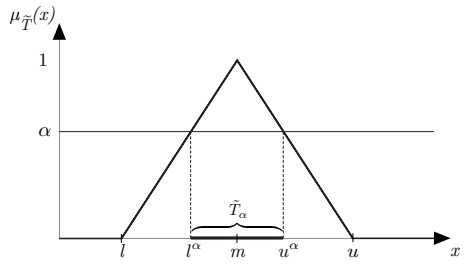

Fig. 1. Membership function of a TFN, and its alpha-cut $\tilde{T}\alpha$.

A *fuzzy number* is a convex and normalized fuzzy set defined on $\mathbb{R}$. *Triangular fuzzy numbers* (TFNs) are widely used to express human judgments. Formally, given $l, m, u \in \mathbb{R}$, such that $l \leq m \leq u$, the membership function $\mu_{\tilde{T}}(x)$ of a TFN $\tilde{T}$, shown in Fig. 1, assumes values such that: $\mu_{\tilde{T}}(x) = 0$ if $x < l \vee x > u$ or $\mu_{\tilde{T}}(x) = \frac{x-l}{m-l}$ if $l \leq x \leq m$ or $\mu_{\tilde{T}}(x) = \frac{u-x}{u-m}$ if $m \leq x \leq u$.

An alternative representation of $\tilde{T}$, based on the interval of confidence (or alpha-cut), is $\tilde{T}_\alpha = [l^\alpha, u^\alpha] = [(m-l)\alpha + l, -(u-m)\alpha + u], \forall \alpha \in [0, 1]$ (see Fig. 1).

Fuzzy AHP (F-AHP) deals with uncertainty and vagueness by substituting the Saaty's scale with a fuzzy version based on TFNs from $\tilde{1}$ to $\tilde{9}$.

More rigorously, let $\tilde{P}$ be an $n \times n$ pairwise comparison matrix containing TFNs $\tilde{p}^\alpha_{ij} = [p^\alpha_{ij_l}, p^\alpha_{ij_u}]$, and let $\tilde{x}$ be a non-zero $n \times 1$ vector containing fuzzy numbers $\tilde{x}_i = [x^\alpha_{i_l}, x^\alpha_{i_u}]$. A fuzzy eigenvalue $\tilde{\lambda}$ is a fuzzy number that is a solution of $\tilde{P}\tilde{x} = \tilde{\lambda}\tilde{x}$. In order to compute the principal

eigenvector, matrix $\tilde{P}$ has to be defuzzified. Defuzzification maps a fuzzy set into a number. There are several ways to perform defuzzification. For instance, $\tilde{P}$ can be defuzzified by introducing a coefficient $\zeta \in [0,1]$, called *index of optimism*, used to perform a convex combination for each element of $\tilde{P}$, obtaining $\hat{P} = [\hat{p}_{ij}^{\alpha}] = [\zeta p_{ij_u}^{\alpha} + (1-\zeta)p_{ij_l}^{\alpha}]$. The principal eigenvector of $\hat{P}$ is then calculated as in classic AHP.

IV. DC Power Flow Model with Losses

A. Overview

Considered an AC transmission line connecting two buses i and j, active and reactive power flows are expressed by:

$$p_{ij} = V_i^2 g_{ij} - V_i V_j (g_{ij}\cos\theta_{ij} + b_{ij}\sin\theta_{ij}) \quad (5)$$

$$q_{ij} = -V_i^2 b_{ij} - V_i V_j (g_{ij}\sin\theta_{ij} + b_{ij}\cos\theta_{ij}). \quad (6)$$

DC models consider voltages and voltage angles expressed in per-unit (p.u.), i.e., fractions of a chosen base unit quantity. DC models make the assumption that active power flow tends to be significantly higher than reactive power flow, i.e., $p_{ij} \gg q_{ij}$: for this reason, only active power is considered. Also, voltage magnitudes are assumed to be close to 1 p.u. (flat voltage profile), and small voltage phase angle differences are supposed. Hence, DC models assume $\sin\theta_{ij} \approx \theta_{ij}$ and $\cos\theta_{ij} \approx 1$, consequently Equation (5) becomes:

$$p_{ij} \approx b_{ij}\theta_{ij} = \frac{\theta_{ij}}{x_{ij}}. \quad (7)$$

Considering two directly connected buses i and j, ohmic losses across the line (i,j) are expressed as the difference between the power sent by bus i and the power received by bus j, obtaining the following well-known loss expression:

$$\ell_{ij} = 2g_{ij}(1-\cos\theta_{ij}). \quad (8)$$

DC power flow basic formulations do not consider transmission losses, since they assume $\cos\theta_{ij} \approx 1$. However, in a large power system, transmission losses cannot be neglected. In this paper, transmission losses are considered in the model through piecewise linearization.

B. Piecewise linear approximation of losses

We approximate losses through a piecewise linearization of the term $\cos\theta_{ij}$ of Equation (8) using secant line segments, as shown in Fig. 2. Usually, mixed integer linear programming

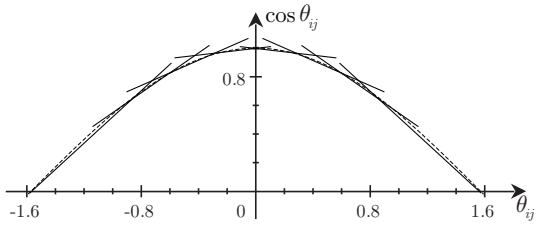

Fig. 2. Cosine (dashed line) and piecewise linear approximation of the cosine (solid lines).

models of losses are used to avoid fictitious losses introduction. Actually, a piecewise linear model does not introduce fictitious losses, if reactive power losses are neglected [31].

V. Model

A. Microgrid

We represent a microgrid by a directed graph wherein a bus is represented as a node and a power line as a directed arc. Nodes are identified by integer numbers and arcs are represented using ordered pairs. Hereafter, buses are also referred to as nodes, and lines as arcs. In Fig. 3, the dotted rectangle contains a microgrid. Nodes within a microgrid can be active or passive. A node is active (passive) if it provides (consumes) energy. A *dispatcher* (depicted in Fig. 3 as a dark

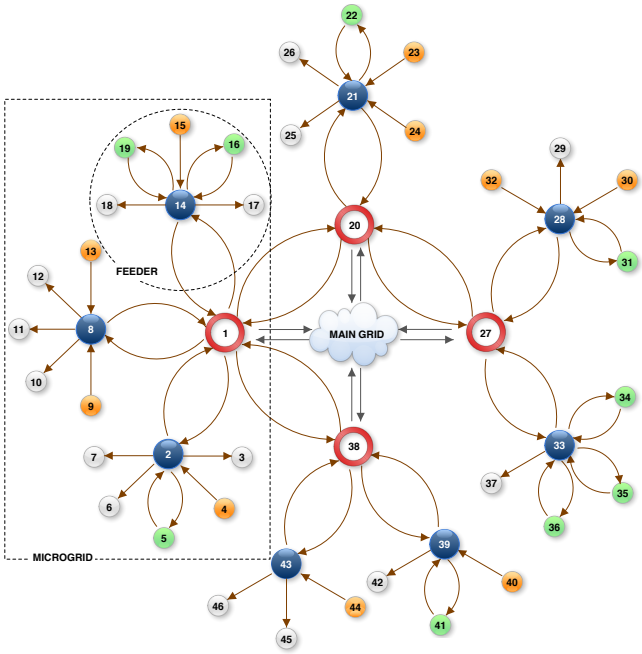

Fig. 3. A simple smart grid represented by a directed graph.

circle with the number in white) is a node which neither consumes nor produces energy. Its task simply consists in dispatching the power available in the active nodes to the passive nodes. Each dispatcher is connected to a node which is called *central controller* (represented in Fig. 3 with a ring) via a pair of arcs: one directed from the dispatcher to the central controller, the other directed in the opposite direction. Like the dispatchers, central controllers neither produce nor consume energy; central controllers are connected to the main grid at the point of common coupling.

A *producer* (a circle having a unique outgoing arc in Fig. 3) is an active node, more precisely a generator, characterized by the distance from the dispatcher to which it is connected (in kilometers), the minimum and maximum suppliable power (in kilowatts), the way by which it generates energy (e.g., fossil fuels, waste, sunlight, wind, etc.), the environmental impact, i.e., the amount of pollutants released into the environment

due to energy production (expressed in tons of pollutants released per kWh), and the cost per kWh of energy provided (in dollars).

A *consumer* (represented in Fig. 3 as a circle having a unique incoming arc) is a passive node, often referred to as a *load*. A consumer is characterized by the distance from the dispatcher (in kilometers), and the nominal power (in kilowatts). Within a smart microgrid, a load can be *sensitive*, *adjustable*, or *shedable*. A sensitive load cannot stop working, hence the nominal power has always to be guaranteed. Differently, an adjustable load works also at power levels below its nominal power. Because of high energy pricing during peak periods, adjustable loads can reduce their power consumption, accomplishing the so-called peak curtailment. Finally, a shedable load requires its nominal power to work, but its switching on can be moved in time depending on energy pricing.

A *prosumer* (in Fig. 3 a circle having a pair of arcs connecting it to a dispatcher) is a node which produces or consumes electricity. At any instant, a prosumer is active if it can supply electricity, otherwise it is passive. A passive prosumer is considered as a load. A prosumer is characterized by all the attributes of producers and consumers. We assume prosumers generate electricity by using renewable sources, thus having a zero environmental impact.

Each producer or consumer is connected to a dispatcher through an arc. In the case of a producer (consumer), the arc has its head in the dispatcher (consumer) and its tail in the producer (dispatcher). Further, each prosumer is connected to a dispatcher through a pair of arcs: one directed to the dispatcher, the other directed to the prosumer.

Microgrids are composed by *feeders*. A feeder includes all the nodes of a microgrid (except its central controller) that are connected to one of its dispatchers, including the dispatcher itself. In Fig. 3 the dotted circle contains a feeder.

B. Smart grid

A smart grid is composed by microgrids, each one having its own central controller.

Two microgrids may be physically connected to each other. In our model this happens if there exists a pair of arcs connecting their central controllers. Further, there always exists a pair of arcs connecting each central controller to the main grid. Each microgrid can work in grid-connected mode or in islanded mode. In the former case, it exchanges energy with the other microgrids. In the latter case, it is disconnected both from the other microgrids and from the main grid. A microgrid working in islanded mode is said to be *islanded*.

VI. Linear programming-driven multi-criteria (LPDM) economic dispatch

A. Energy dispatch: an overview

Energy dispatch is generally performed in two steps: unit commitment (UC) and economic dispatch (ED). Within a smart grid, there are dispatchable and non-dispatchable generators: the former are traditional generators (e.g., generators based on fossil fuels, incineration of waste, biomass, and so on) whose energy production level is deterministic; the latter are based on renewable sources, thus subject to uncertainty concerning the effective power produced at a given time in the future. UC determines the scheduled generators, that is, the dispatchable generators that have to be active within a given hour of the next day to meet the forecasted load for that hour of the next day. Subsequently, ED performs a short-term determination (minutes or hours ahead) of the power output of scheduled and non-dispatchable generators, and active prosumers to meet the actual load, under operational constraints, minimizing the energy cost.

B. Description of the LPDM optimization technique

Our optimization process aims to minimize environmental impact, cost of the energy, distance of supply, and to optimize the load balancing by distributing the total load over the power lines. We do not consider transmission losses minimization as a further objective; however, by considering load balancing as objective, also transmission losses are implicitly controlled. The problem is addressed through an LP-driven MCDM approach using a hybrid technique based on fuzzy AHP and TOPSIS. Fuzzy AHP is exploited to rank the criteria on the basis of judgements expressed by the decision maker in terms of triangular fuzzy numbers. Criteria are then heuristically split into two classes corresponding to more important and less important objectives (called, respectively, *driving objectives* and *marginal objectives* from now on) based on the ranking resulting from fuzzy AHP. The weights of the driving objectives are exploited to build the objective function of an LP problem, called *driving problem*, as a normalized weighted sum of the driving objectives, thus making the problem single-objective. The optimal solution (called *driving solution*) serves as a starting point to obtain suboptimal solutions that improve the marginal objectives. Obviously, suboptimal solutions must belong to the Pareto front, hence, as stated in Section II-B, they can be worse than the driving solution (i.e., with respect to the driving objectives) only if they outperform it with respect to, at least, one of the marginal objectives. Such solutions and the driving solution form the *alternatives* of the decision problem. Alternatives are compared by using TOPSIS to choose the one becoming the new power output configuration for the scheduled generators and the non-dispatchable electricity generation facilites.

C. Objective functions

Let $p \in \mathbb{R}_+^{|\mathcal{L}|}$, where $|\cdot|$ indicates the cardinality, be a feasible power flow configuration over the power lines. We model the energy cost as a piecewise approximation of the following cost function, where $c_{i,\alpha}$, $c_{i,\beta}$ and $c_{i,\gamma}$ are the cost coefficients of generator i:

$$c(p) = \sum_{i \in \mathcal{G} \cup \mathcal{A}} \sum_{j \in \mathcal{B}_i^{\rightarrow}} c_{i,\alpha} + c_{i,\beta} p_{ij} + c_{i,\gamma} p_{ij}^2. \qquad (9)$$

Likewise, we model the environmental impact through piecewise approximation of the following quadratic emission func-

tion [32], where $\pi_{i,\alpha}$, $\pi_{i,\beta}$ and $\pi_{i,\gamma}$ are coefficients related to the emission characteristics of the i-th generator:

$$\pi(p) = \sum_{i \in \mathcal{G}} \sum_{j \in \mathcal{B}_i^{\rightarrow}} \pi_{i,\alpha} + \pi_{i,\beta} p_{ij} + \pi_{i,\gamma} p_{ij}^2. \tag{10}$$

The distance of supply is modeled as

$$d(p) = \sum_{(i,j) \in \mathcal{L}} d_{ij} p_{ij}, \tag{11}$$

and the load level of the power lines as

$$l(p) = \frac{1}{|\mathcal{L}|} \sum_{(i,j) \in \mathcal{L}} \frac{p_{ij}}{\overline{\varphi}_{ij}}, \tag{12}$$

where $\pi : \mathbb{R}_+^{|\mathcal{G}|} \to \mathbb{R}$, c, $d : \mathbb{R}_+^{|\mathcal{L}|} \to \mathbb{R}$, $l : \mathbb{R}_+^{|\mathcal{L}|} \to (0, 1]$.

D. Ranking of the objectives

The ranking of the objectives is performed by fuzzy AHP, as described in Section III-B. In order to automatically determine the driving objectives we use the K-means algorithm [33], one of the most popular clustering techniques. We apply the K-means algorithm to the weights in w. In our scenario we aim to split the objectives into two classes of importance, driving and marginal, hence we consider K, i.e., the number of clusters, equal to 2. On the other hand, it may make little sense to split the objectives into two classes whenever their weights are rather uniformly distributed. In such a case, there does not exist a clear preference for a specific subset of the objectives. The perfect uniform distribution of four weights summing to one is $w^{unif} = (0.25, 0.25, 0.25, 0.25)$. We define a ball centered in w^{unif}, having radius $\tau > 0$, $B_\tau(w^{unif}) = \{w \in \mathbb{R}^4 : (\sum_{i=1}^4 (w_i - w_i^{unif})^2)^{0.5} \leq \tau\}$. The radius of the ball is heuristically chosen to represent the minimum distance from perfect uniform distribution, beyond which a configuration of weights is allowed to be processed by the K-means algorithm. More rigorously, given a ranking of the weights of the objectives w^{rank} resulting from fuzzy AHP, the K-means algorithm is applied only if $w^{rank} \notin B_\tau(w^{unif})$.

E. Driving problem formulation

Let us consider a directed graph representing a smart grid as explained in Section V. Let $\mathcal{D}$ be the set of the driving objectives, and let f_i be the objective function of the i-th driving objective, where $i \in \mathcal{D}$. The model of the driving problem is the following:

$$\text{Minimize } \; z = \sum_{i \in \mathcal{D}} \omega_i N_{[0,1]} \left(f_i(p) \right) \tag{13a}$$

subject to:

$$\sum_{j \in \mathcal{B}_i^{\leftarrow}} (p_{ji} - \ell_{ji}) - \sum_{j \in \mathcal{B}_i^{\rightarrow}} (p_{ij} + \ell_{ij}) = 0, \; \forall i \in \mathcal{B} \tag{13b}$$

$$p_{ij} = \frac{\theta_{ij}}{x_{ij}}, \; \forall (i,j) \in \mathcal{L} \tag{13c}$$

$$\ell_{ij} = 2 g_{ij} \left(1 - \min_{k \in \{1, \ldots, NS\}} a_k \theta_{ij} + b_k \right), \; \forall (i,j) \in \mathcal{L} \tag{13d}$$

$$0 \leq p_{ij} \leq \overline{\varphi}_{ij}, \; \forall (i,j) \in \mathcal{L} \tag{13e}$$

$$\sum_{j \in \mathcal{B}_i^{\rightarrow}} p_{ij} \leq \overline{P_i}, \; \forall i \in \mathcal{A} \tag{13f}$$

The objective function in Equation (13a), is a normalized weighted sum of the driving objectives, where $\omega_i = \frac{w_i}{\sum_{i \in \mathcal{D}} w_i}$, w_i is the weight of the i-th objective obtained by fuzzy AHP, and $N_{[0,1]}$ is a normalization function to scale the values of all the objective functions in the same range, in this case, the interval $[0, 1]$. Given an objective function f_i, where $i \in \mathcal{D}$, the normalization function $N_{[0,1]}$ is defined as:

$$N_{[0,1]}(f_i(p)) = \frac{f_i(p) - \min(f_i(p))}{\max(f_i(p)) - \min(f_i(p))}. \tag{14}$$

Constraints in (13b) are the active power balance at all buses. Equation (13c) is the expression of the power flow on each line (i, j) in terms of the voltage phase angle difference θ_{ij} between buses i and j. Equation (13d) is the piecewise linear approximation (performed by using NS segments) for the power losses of each line, where a_k and b_k are, respectively, the slope and the y-intercept of the k-th segment. Constraints (13e) force the power flow on each line to be lower than its maximum sustainable flow. Upper active power limits of the active prosumer are in Equation (13f).

F. Alternative generation

Once the driving solution is computed, marginal objectives have to be taken into account in order to generate Pareto-optimal solutions (alternatives) that improve one (or possibly more) of them. Note that in all this section we will use the matrix notation. Let n be the number of marginal objectives, let $M \in \mathbb{R}_+^{n \times |\mathcal{L}|}$ be a matrix wherein each row m_k contains the coefficients of the k-th marginal objective function, with $k \in \{1, \ldots, n\}$, and let $z \in \mathbb{R}_+^{|\mathcal{L}|}$ contain the coefficients of the driving objective function. In this section, for simplicity, we will use the symbol m_k also to refer to the k-th marginal objective function. Also, let $\hat{p} \in \mathbb{R}_+^{|\mathcal{L}|}$ be the driving solution. At first, we might consider the antigradient of each marginal objective function at the driving solution, i.e., $-\nabla m_k \hat{p}^T = \left(-\frac{\partial m_k}{\partial p_1}, -\frac{\partial m_k}{\partial p_2}, \ldots, -\frac{\partial m_k}{\partial p_{|\mathcal{L}|}} \right) \hat{p}^T$. However, since the objective functions have non-negative coefficients, their gradients have all positive (or zero) components, hence it is impossible to improve a marginal objective at the driving solution $\hat{p}$, by moving through the directions $-\nabla m_k \hat{p}^T, \forall k \in \{1 \ldots n\}$. A simple two-dimensional graphic representation of alternative generation is shown in Fig. 4. Here, we consider two producers D and E, and a consumer F, so that p_{DF} and p_{EF} represent the power flow on the lines (D, F) and (E, F), respectively. Our technique improves each marginal objective m_k by moving the driving solution through the directions obtained by the orthogonal projection of each antigradient $-\nabla m_k$ onto the subspace generated by the active constraints at the driving solution. A constraint is said to be active at a solution if it holds with equality at the solution itself. Let us consider the problem (13a-13f) in the standard form $\min\{z^T p \,|\, Ap \leq b, p \geq 0\}$, by

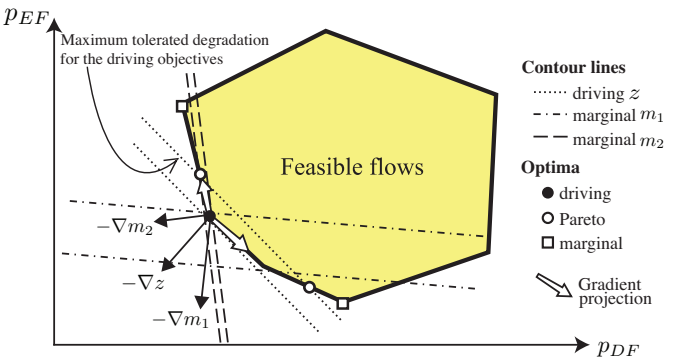

Fig. 4. Two-dimensional representation of the generation of alternatives of a problem having two marginal objectives.

supposing the use of slack variables where needed, where A is the coefficient matrix of the constraints and b is the vector of the constant terms. Let C contain the rows of A related to active constraints at $\hat{p}$. The orthogonal projection of $-\nabla m_k$ onto the subspace generated by the active constraints at $\hat{p}$ is $-H\nabla m_k \hat{p}^T$, where $H = I - C^T(CC^T)^{-1}C$. By moving the driving solution through such directions, Pareto-optimal solutions are guaranteed to be generated, because, even though the driving objectives are degraded, the marginal objectives are unconditionally improved. However, it is important to note that a degradation of the driving objective function (13a) does not necessarily correspond to a degradation of all the driving objectives. In fact, alternative generation might even improve one or more of the driving objectives, depending on the gradient orientation of their own objective function.

In any case, each marginal objective m_k is improved while keeping, at the same time, the value of the driving objective function lower than a specified degradation threshold. Let $\xi > 0$ be the maximum percentage degradation tolerated for the driving objective function, hence, Pareto-optimal alternatives $p \in \mathbb{R}_+^{|\mathcal{L}|}$ such that $zp^T > \overline{z}$, where $\overline{z} = (1 + 0.01\xi)z\hat{p}^T$, are not accepted. During alternative generation, whenever a new vertex is reached, the orthogonal projection of $-\nabla m_k$ onto the subspace generated by the new active constraints is recomputed. Anyway, if the vertex reached is the optimum of m_k (called *marginal optimum*), the generation of alternatives improving m_k ends: m_k cannot be improved anymore. In such a case, the marginal optimum is considered as an alternative. Algorithm 1 shows the pseudocode of alternative generation.

G. Alternative selection

The *TOPSIS* algorithm compares the alternatives by using the objective functions defined in Section VI-C, according to the weights of the criteria obtained as described in Section VI-D, and chooses the best one.

VII. Simulation results

The linear programming-driven multi-criteria technique (LPDM) has been implemented in MATLAB®. In this section we will discuss the results we obtained by testing the LPDM technique on the prototype 20-kV smart microgrid whose central controller is labelled with 1, in Fig. 3. Table II contains length, resistance (R) and reactance (X) of each line of the tested microgrid. The parameters characterizing each load, i.e., the position, the nominal apparent power, and the power factor are summarized in Table III. Table IV shows the power limit of generators and active prosumers. The hourly energy cost per kilowatt (in dollars) and the hourly pollutant emission per kilowatt (in tons) are summarized in Table V. We recall that the objectives are the load balancing (L), the cost of the energy (C), the distance of supply (D), and the environmental impact (E). Judgements for pairwise comparisons should be expressed by an expert. Nevertheless, based on heuristic considerations, we estimated them by adding uncertainty through triangular fuzzy numbers having a support with length equal to 2.

We performed diverse pairwise comparisons to simulate a set of situations wherein the objectives assume different priorities, in order to investigate the performance of the LPDM technique with respect to the importance assigned to the objectives. We heuristically set the index of optimism ζ of our judgements to 0.4. For reasons of space, pairwise comparison matrices are omitted. However, each configuration of weights we used for the simulations is shown as a row in Table VI. Simulations were carried out by testing the LPDM technique in 40 scenarios, representing possible real-world situations, obtained by combining each weight configuration in Table VI with all the operating conditions in Table VII. To guarantee

Algorithm 1 Alternative generation

1: **INPUT:** $\hat{p}, M, n, z, \overline{z}$
2: **OUTPUT:** PA (matrix of the Pareto alternatives)
3: $p \leftarrow \hat{p}$
4: $k \leftarrow 1$
5: **while** $k \leq n$ **do**
6: Find the active constraints at p, $\mathcal{Q} \leftarrow \{i : A_i p = b_i\}$
7: Construct the matrix C of the rows A_i, $\forall i \in \mathcal{Q}$
8: Set the projection matrix $H \leftarrow I - C^T(CC^T)^{-1}C$
9: $d \leftarrow -H\nabla m_k p^T$
10: **if** $d = 0$ **then**
11: $k \leftarrow k + 1$
12: insert p into PA and go to line 5
13: **else**
14: Let $t^{\max}$ be the solution of: $\begin{cases} \max t \\ A(p + td) \leq b \end{cases}$
15: Compute $t^\star \leftarrow \underset{\substack{t\in[0,t^{\max}] \\ z(p+td)\leq\overline{z}}}{\arg\min}\ m_k(p + td)$
16: $p \leftarrow (p + t^\star d)$
17: **if** $\mathrm{rank}(C) < |\mathcal{L}|$ (i.e., p is not a vertex) **then**
18: $k \leftarrow k + 1$
19: insert p into PA and go to line 5
20: **else**
21: go to line 6
22: **end if**
23: **end if**
24: **end while**

TABLE II
LINE PARAMETERS OF THE TESTED MICROGRID

Line	Length	R(Ω)	X(Ω)
(1,2)	3	0.579	0.329
(1,8)	3	0.579	0.329
(1,14)	3	0.579	0.329
(2,1)	0.5	0.097	0.055
(2,3)	2	0.386	0.219
(2,5)	1	0.193	0.109
(2,6)	1	0.193	0.109
(2,7)	1.5	0.289	0.165
(4,2)	0.5	0.097	0.055
(5,2)	1	0.193	0.109
(8,1)	0.5	0.097	0.055
(8,10)	1	0.193	0.109
Line	**Length**	**R(Ω)**	**X(Ω)**
(8,11)	2	0.386	0.219
(8,12)	0.5	0.097	0.055
(9,8)	1	0.193	0.109
(13,8)	2	0.386	0.219
(14,1)	1	0.193	0.109
(14,16)	1.5	0.289	0.165
(14,17)	1.5	0.289	0.165
(14,18)	1	0.193	0.109
(14,19)	1	0.193	0.109
(15,14)	1	0.193	0.109
(16,14)	1.5	0.289	0.165
(19,14)	1	0.193	0.109

TABLE III
LOAD PARAMETERS

Node	S(kVA)	cosϕ
3	600	0.95
7	850	0.97
8	550	0.95
10	600	0.97
11	800	0.95
Node	**S(kVA)**	**cosϕ**
12	730	0.95
17	600	0.95
18	800	0.95
19	650	0.95

TABLE IV
POWER LIMITS OF GENERATORS (LEFT) AND ACTIVE PROSUMERS (RIGHT)

Node	S(kVA)	$\overline{P}$(kW)
4	5000	4000
9	3750	3000
13	6250	5000
15	5000	4000

Node	S (kVA)	cosϕ
5	450	1
16	500	1

TABLE V
HOURLY COST OF THE ACTIVE POWER AND POLLUTANT EMISSIONS

Node	Cost ($/kWh)	Emission (t/kWh)
4	0.185	0,0081272
9	0.191	0,0078521
13	0.175	0,0071053
15	0.169	0,0075005

a reasonable trade-off between approximation accuracy and number of constraints (13d), transmission losses have been approximated by using four segments linearizing the term $\cos\theta_{ij}$ of Equation (8). In all the scenarios, we tolerated a

TABLE VI
WEIGHT CONFIGURATIONS OF THE CRITERIA

w_L	w_C	w_D	w_E
0.132	0.381	0.434	0.053
0.122	0.531	0.326	0.021
0.215	0.101	0.339	0.345
0.292	0.105	0.01	0.593
0.46	0.38	0.1	0.06
0.263	0.197	0.247	0.293
0.731	0.037	0.142	0.09
0.102	0.075	0.105	0.718

TABLE VIII
PERCENTAGE DIFFERENCES OF THE FOUR OBJECTIVES BETWEEN THE OPTIMAL SOLUTIONS OBTAINED BY LPDM AND WS

Block	**Weights**	**(0.132, 0.381, 0.434, 0.053)**			
	Op. conditions	ΔL	ΔC	ΔD	ΔE
1	1	25.12%	-0.28%	8.16%	-8.83%
	2	40.8%	-0.65%	7.63%	-9.8%
	3	41.19%	-0.75%	12.37%	-10.3%
	4	29.33%	-0.34%	8.55%	-8.92%
	5	27.1%	-0.7%	7.84%	-10.1%
Block	**Weights**	**(0.122, 0.531, 0.326, 0.021)**			
	Op. conditions	ΔL	ΔC	ΔD	ΔE
3	1	32.5%	-0.68%	7.34%	-15.7%
	2	45.74%	-0.88%	2.79%	-16.4%
	3	49.31%	-0.95%	10.6%	-19.3%
	4	33.7%	-0.77%	7.21%	-14.29%
	5	36.53%	-0.86%	8.39%	-17.28%
Block	**Weights**	**(0.215, 0.101, 0.339, 0.345)**			
	Op. conditions	ΔL	ΔC	ΔD	ΔE
5	1	3.26%	-0.24%	4.22%	-0.41%
	2	8.32%	-1.49%	3.75%	-0.62%
	3	9.17%	-2.01%	5.91%	-1.55%
	4	3.45%	-0.52%	4.28%	-0.39%
	5	7.53%	-1.96%	5.28%	-1.28%
Block	**Weights**	**(0.292, 0.105, 0.01, 0.593)**			
	Op. conditions	ΔL	ΔC	ΔD	ΔE
7	1	6.68%	1.42%	-48.33%	4.27%
	2	5.49%	1.27%	-42.41%	3.98%
	3	5.91%	1.95%	-49.16%	5.29%
	4	5.15%	1.82%	-33.37%	5.27%
	5	5.33%	1.86%	-40.81%	4.12%

Block	**Weights**	**(0.46, 0.38, 0.1, 0.06)**			
	Op. conditions	ΔL	ΔC	ΔD	ΔE
2	1	5.77%	-1.36%	11.2%	-8.56%
	2	7.31%	-2.07%	9.92%	-9.08%
	3	9.35%	-2.14%	10.89%	-9.71%
	4	5.94%	-1.46%	10.43%	-7.95%
	5	8.82%	-1.29%	9.24%	-9.97%
Block	**Weights**	**(0.263, 0.197, 0.247, 0.293)**			
	Op. conditions	ΔL	ΔC	ΔD	ΔE
4	1	0.49%	-0.22%	0.08%	-0.13%
	2	0.57%	-0.31%	0.16%	-0.13%
	3	0.59%	-0.46%	0.24%	-0.19%
	4	0.09%	-0.12%	0.04%	-0.06%
	5	0.51%	-0.38%	0.18%	-0.13%
Block	**Weights**	**(0.731, 0.037, 0.142, 0.09)**			
	Op. conditions	ΔL	ΔC	ΔD	ΔE
6	1	115.4%	-0.33%	5.76%	-5.22%
	2	118.2%	-0.52%	5.98%	-7.61%
	3	118.2%	-0.52%	5.98%	-7.61%
	4	100.8%	-0.29%	5.38%	-6.21%
	5	115.9%	-0.46%	4.18 %	-6.92%
Block	**Weights**	**(0.102, 0.075, 0.105, 0.718)**			
	Op. conditions	ΔL	ΔC	ΔD	ΔE
8	1	2.45%	-24.55%	6.22%	4.71%
	2	2.18%	-23.72%	6.03%	4.52%
	3	2.36%	-24.69%	6.57%	4.78%
	4	2.16%	-21.71%	5.93%	4.62%
	5	2.28%	-22.72%	6.15%	4.83%

TABLE VII
TESTED OPERATING CONDITIONS

Identifier	Load demand	Generators and active prosumers status					
		4	9	13	15	5	16
1	100%	OFF	ON	ON	ON	100 %	100%
2	100%	ON	OFF	ON	OFF	100%	85%
3	80%	ON	ON	OFF	ON	94%	10 %
4	75%	OFF	OFF	ON	ON	80%	75%
5	70%	ON	OFF	ON	OFF	75%	100%

maximum degradation of the driving objectives of 10%. Also, we set the radius of the ball preventing the application of the K-means to 0.2. We compared the solution obtained by the LPDM technique with the one obtained by the weighted sum (WS) method, a widely used a priori multi-objective optimization technique, aiming to highlight the overall improvement which can be obtained with LPDM. To compare the results achieved by the WS method and the LPDM technique we used the percentage difference. Table VIII shows the comparisons between the LPDM technique and the WS method in each scenario as percentage differences. For understandability, since we deal with a minimization problem, in the table we reversed the signs of the percentage differences, so that a positive sign indicates an improvement and a negative sign indicates a degradation of an objective function. The table is organized in blocks, numbered from 1 to 8. Each block contains the values of the above percentage differences in the scenarios obtained by combining the weight configuration in the header of the block with the operating conditions specified in the first column of the block. In the header of each block the weights of the driving objectives are underlined.

To help the reader interpret the table, let us refer to the first row of block 1 in Table VIII. This row contains the percentage differences between LPDM and WS for the four objectives in the scenario identified by the weights $w_L = 0.132$, $w_C = 0.381$, $w_D = 0.434$, $w_E = 0.053$ under the operating conditions 1. These percentage differences are obtained from the results achieved by the LPDM technique and the WS method for this scenario (see Table IX). Please note that, for the sake of clarity, in Table IX we have adopted the notation $p_{(i,j)}$ to refer to the power flow on line (i, j).

In Table IX, the first six rows contain the power flow injected by the four generators and the two active prosumers, respectively. The last four rows of the table show the performance values obtained by the LPDM technique and the WS method for all the objectives.

The simulation results shown in Table VIII indicate that, in all the tested scenarios, the LPDM technique is able to produce solutions comparing favourably with the WS method. Indeed, the following situations may occur: i) the solution generated by LPDM significantly improves the most important marginal objective by slightly penalizing one of the driving objectives (see blocks 1, 2, 3 and 5 in Table VIII); ii) the solution generated by LPDM significantly degrades the least important marginal objective by modestly improving all the other (driving and marginal) objectives (see blocks 7 and 8 in Table VIII); iii) the solution generated by LPDM shows a significant improvement and a modest improvement of, respectively, the only driving objective and the most important marginal objective by slightly/modestly degrading the other marginal objectives (see block 6 in Table VIII). Of course, the LPDM technique shows to be better than the WS method whenever there is a clear separation between the driving objectives and the marginal objectives. Intuitively, this occurs when the least important driving objective is characterized by a weight significantly far from the one assigned to the most important marginal objective.

On the other hand, when a separating border between the driving and the marginal objectives is hard to establish, the LPDM technique tends to substantially behave as the WS method (see block 4 in Table VIII).

TABLE IX
POWER FLOWS FROM GENERATORS AND ACTIVE PROSUMERS OF THE SOLUTIONS OBTAINED BY LPDM AND WS UNDER OPERATING CONDITIONS 1 AND WEIGHTS $(0.132, 0.381, 0.434, 0.053)$

	LPDM	WS
$p_{(4,2)}$ (kW)	0	0
$p_{(9,8)}$ (kW)	3000	3000
$p_{(13,8)}$ (kW)	0	0
$p_{(15,14)}$ (kW)	2450.21	1950.32
$p_{(5,2)}$ (kW)	450.37	450.96
$p_{(16,14)}$ (kW)	0	0
Emissions (t)	41.9	38.2
Cost ($)	1063.6	1063.3
Distance (km)	3783	3866.4
Load level (%)	43.55	58.16

VIII. CONCLUSION

In this paper we have proposed the LPDM technique, a novel approach to multi-objective optimization of energy dispatch in smart grids considering the environmental impact, the energy cost, the distance of supply, and the load balancing as objectives. Objectives are ranked by means of fuzzy AHP, by exploiting judgements expressed through triangular fuzzy numbers. The main novelty of our work consists in structuring the multi-objective optimal power flow problem as a multi-criteria decision making problem whose alternatives, i.e., Pareto-optimal power flow configurations, are dynamically and automatically generated by exploiting the optimal solution to an LP driving problem which considers the most important criteria as objectives. Alternatives are finally evaluated with respect to all the objectives by using TOPSIS.

The LPDM technique has been validated by simulating 40 scenarios on a prototype microgrid. Simulation results have shown that the LPDM technique compares favourably with the WS method in all the tested scenarios. Indeed, the optimal power flows produced by LPDM show, with respect to those generated by WS, one of the following characteristics: i) a significant improvement of the most important marginal objective by slightly penalizing one of the driving objectives; ii) a significant degradation of the least important marginal objective by modestly improving all the other (driving and

marginal) objectives; iii) a significant improvement of the only driving objective and, at the same time, a modest improvement of the most important marginal objective, by slightly/modestly degrading the other marginal objectives.

The degree of improvement of LPDM with respect to WS is obviously dependent on the configuration of weights and the operating conditions of the microgrid. The lowest degree of improvement is achieved when the weights are too uniformly distributed among the objectives, meaning there is not a clear preference for a specific subset of the objectives. In fact, when this happens, it makes no sense to single out the driving objectives at all. This situation is probably not so common in real-world scenarios, especially when the number of objectives increases; nevertheless, in such a case, LPDM just behaves as the WS method.

REFERENCES

[1] V. C. Gngr, D. Sahin, T. Kocak, S. Ergt, C. Buccella, C. Cecati, and G. P. Hancke, "Smart grid technologies: Communication technologies and standards," *IEEE Trans. Ind. Inf.*, vol. 7, no. 4, pp. 529–539, 2011.

[2] F. Kennel, D. Grges, and S. Liu, "Energy management for smart grids with electric vehicles based on hierarchical mpc," *IEEE Trans. Ind. Inf.*, vol. 9, no. 3, pp. 1528–1537, 2013.

[3] C.-I. Fan, S.-Y. Huang, and Y.-L. Lai, "Privacy-enhanced data aggregation scheme against internal attackers in smart grid," *IEEE Trans. Ind. Inf.*, vol. 10, no. 1, pp. 666–675, 2014.

[4] J. Navarro, A. Zaballos, A. Sancho-Asensio, G. Ravera, and J. Armendariz-Inigo, "The information system of integris: Intelligent electrical grid sensor communications," *IEEE Trans. Ind. Inf.*, vol. 9, no. 3, pp. 1548–1560, 2013.

[5] A. J. D. Rathnayaka, V. M. Potdar, T. S. Dillon, O. K. Hussain, and E. Chang, "A methodology to find influential prosumers in prosumer community groups," *IEEE Trans. Ind. Inf.*, vol. 10, no. 1, pp. 706–713, 2014.

[6] B. Bahrani, M. Saeedifard, A. Karimi, and A. Rufer, "A multivariable design methodology for voltage control of a single-dg-unit microgrid," *IEEE Trans. Ind. Inf.*, vol. 9, no. 2, pp. 589–599, 2013.

[7] I. J. Balaguer, S. Y. Qin Lei, U. Supatti, and F. Z. Peng, "Control for grid-connected and intentional islanding operations of distributed power generation," *IEEE Trans. Ind. Electron.*, vol. 58, no. 1, pp. 147–157, 2011.

[8] F. D. Angelis, M. Boaro, D. Fuselli, S. S. andFrancesco Piazza, and Q. Wei, "Optimal home energy management under dynamic electrical and thermal constraints," *IEEE Trans. Ind. Inf.*, vol. 9, no. 3, pp. 1518–1527, 2013.

[9] P. Siano, C. Cecati, H. Yu, and J. Kolbusz, "Real time operation of smart grids via fcn networks and optimal power flow," *IEEE Trans. Ind. Inf.*, vol. 8, no. 4, pp. 944–952, 2012.

[10] L. F. Ochoa and G. P. Harrison, "Minimizing energy losses: Optimal accommodation and smart operation of renewable distributed generation," *IEEE Trans. Power Syst.*, vol. 26, no. 1, pp. 198–205, 2011.

[11] Y. M. Atwa, E. F. El-Saadany, M. M. A. Salama, and R. Seethapathy, "Optimal renewable resources mix for distribution system energy loss minimization," *IEEE Trans. Power Syst.*, vol. 25, no. 1, pp. 360–370, 2010.

[12] V. Bakker, M. Bosman, A. Molderink, J. Hurink, and G. Smit, "Demand side load management using a three step optimization methodology," in *Proc. IEEE SmartGridComm*, 2010, pp. 431–436.

[13] L. Chen, N. Li, S. H. Low, and J. C. Doyle, "Two market models for demand response in power networks," in *Proc. IEEE SmartGridComm*, 2010, pp. 397–402.

[14] S. Ghosh, J. Kalagnanam, D. Katz, M. Squillante, X. Zhang, and E. Feinberg, "Incentive design for lowest cost aggregate energy demand reduction," in *Proc. IEEE SmartGridComm*, 2010, pp. 519–524.

[15] C. Ibars, M. Navarro, and L. Giupponi, "Distributed demand management in smart grid with a congestion game," in *Proc. IEEE SmartGridComm*, 2010, pp. 495–500.

[16] A. J. Conejo, J. M. Morales, and L. Baringo, "Real-time demand response model," *IEEE Trans. Smart Grid*, vol. 1, no. 3, pp. 236–242, 2010.

[17] X. Guan, Z. Xu, and Q.-S. Jia, "Energy-efficient buildings facilitated by microgrid," *IEEE Trans. Smart Grid*, vol. 1, no. 3, pp. 243–252, 2010.

[18] S. Han, S. Han, and K. Sezaki, "Development of an optimal vehicle-to-grid aggregator for frequency regulation," *IEEE Trans. Smart Grid*, vol. 1, no. 1, pp. 65–72, 2010.

[19] X. Liu, "Economic load dispatch constrained by wind availability: A wait-and-see approach," *IEEE Trans. Smart Grid*, vol. 1, no. 3, pp. 347–355, 2010.

[20] B. Ramachandran, S. K. Srivastava, C. S. Edrington, and D. A. Cartes, "An intelligent auction scheme for smart grid market using a hybrid immune algorithm," *IEEE Trans. Ind. Electron.*, vol. 58, no. 10, pp. 4603–4612, 2011.

[21] X. Liu and W. Xu, "Minimum emission dispatch constrained by stochastic wind power availability and cost," *IEEE Trans. Power Syst.*, vol. 25, no. 3, pp. 1705–1713, 2010.

[22] A. Y. Saber and G. K. Venayagamoorthy, "Plug-in vehicles and renewable energy sources for cost and emission reductions," *IEEE Trans. Ind. Electron.*, vol. 58, no. 4, pp. 1229–1238, 2011.

[23] A.-H. Mohsenian-Rad and A. Leon-Garcia, "Optimal residential load control with price prediction in real-time electricity pricing environments," *IEEE Trans. Smart Grid*, vol. 1, no. 2, pp. 120–133, 2010.

[24] A.-H. Mohsenian-Rad, V. W. S. Wong, J. Jatskevich, R. Schober, and A. Leon-Garcia, "Autonomous demand-side management based on game-theoretic energy consumption scheduling for the future smart grid," *IEEE Trans. Smart Grid*, vol. 1, no. 3, pp. 320–331, 2010.

[25] B. Lazzerini and F. Pistolesi, "Efficient energy dispatching in smart microgrids using an integration of fuzzy ahp and topsis assisted by linear programming," in *Proc. 8th Conference of European Society for Fuzzy Logic and Technology (EUSFLAT)*, 2013, pp. 310–317.

[26] R. T. Marler and J. S. Arora, "Survey of multi-objective optimization methods for engineering," *Struct. Multidisc. Optim.*, vol. 26, no. 6, pp. 369–395, 2004.

[27] B. Lazzerini and F. Pistolesi, "Neural network-based objectives prioritization for multi-objective economic dispatch in microgrids," in *Proc. IEEE/SICE Int. Symp. on System Integration (SII 2014)*, Tokyo, JP, 2014, pp. 665–671. [Online]. Available: http://dx.doi.org/10.13140/2.1.5142.0960

[28] T. Saaty, "How to make a decision: The analytic hierarchy process," *European Journal of Operational Research*, no. 48, pp. 9–26, 1990.

[29] T. L. Saaty, "Decision-making with the ahp: Why is the principal eigenvector necessary," *European Journal of Operational Research*, vol. 145, pp. 85–91, 2003.

[30] L. A. Zadeh, "Fuzzy sets," *Information and Control*, vol. 8, no. 3, pp. 338–353, 1965.

[31] H. Zhang, V. Vittal, G. T. Heydt, and J. Quintero, "A relaxed ac optimal power flow model based on taylor series," in *Proc. Innovative Smart Grid Technology (ISGT)*, 2013.

[32] J. Cai, X. Ma, Q. Li, L. Li, and H. Peng, "A multi-objective chaotic ant swarm optimization for environmental/economic dispatch," *International Journal of Electrical Power & Energy Systems*, vol. 32, no. 5, pp. 337–344, 2010.

[33] J. Macqueen, "Some methods for classification and analysis of multivariate observations," in *Proc. Fifth Berkeley Symp. on Math. Statist. and Prob.*, vol. 1, 1967.